Yarahmadi et al., *BioImpacts.* 2025;15:30272
doi: 10.34172/bi.30272
https://bi.tbzmed.ac.ir/

Automatic classification of *Giardia* infection from stool microscopic images using deep neural networks

Pezhman Yarahmadi[1], Ehsan Ahmadpour[2], Parham Moradi[3], Nasser Samadzadehaghdam[1*]

[1]Department of Biomedical Engineering, Faculty of Advanced Medical Sciences, Tabriz University of Medical Sciences Tabriz, Iran
[2]Department of Parasitology and Mycology, Faculty of Medicine, Tabriz University of Medical Sciences, Tabriz, Iran
[3]Department of Computer Engineering, University of Kurdistan, Sanandaj, Iran

Article Info

Article Type:
Original Article

Article History:
Received: 14 Jan. 2024
Revised: 23 Apr. 2024
Accepted: 28 May 2024
ePublished: 24 Sep. 2024

Keywords:
Giardiasis
Classification
Machine learning
Deep neural network

Abstract

Introduction: Giardiasis is a common intestinal infection caused by the *Giardia* lamblia parasite, and its rapid and accurate diagnosis is crucial for effective treatment. The automatic classification of *Giardia* infection from stool microscopic images plays a vital role in this diagnosis process. In this study, we applied deep learning-based models to automatically classify stool microscopic images into three categories, namely, normal, cyst, and trophozoite.

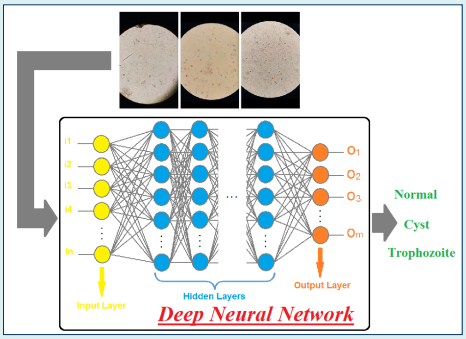

Methods: Unlike previous studies focused on images acquired from drinking water samples, we specifically targeted stool samples. In this regard, we collected a dataset of 1610 microscopic digital images captured by a smartphone with a resolution of 2340 × 1080 pixels from stool samples under the Nikon YS100 microscope. First, we applied CLAHE (Contrast Limited Adaptive Histogram Equalization) histogram equalization a method to enhance the image quality and contrast. We employed three deep learning models, namely Xception, ResNet-50, and EfficientNet-B0, to evaluate their classification performance. Each model was trained on the dataset of microscopic images and fine-tuned using transfer learning techniques.

Results: Among the three deep learning models, EfficientNet-B0 demonstrated superior performance in classifying *Giardia* lamblia parasites from stool microscopic images. The model achieved precision, accuracy, recall, specificity, and F1-score values of 0.9599, 0.9629, 0.9619, 0.9821, and 0.9607, respectively.

Conclusion: The EfficientNet-B0 showed promising results in accurately identifying normal, cyst, and trophozoite forms of *Giardia* lamblia parasites. This automated classification approach can provide valuable assistance to laboratory science experts and parasitologists in the rapid and accurate diagnosis of giardiasis, ultimately improving patient care and treatment outcomes.

Introduction

Every year, around 525 000 children under the age of five die as a result of diarrheal disease, making it the second leading cause of death in this age group.[1] Diarrheal disease stands as a significant cause of both child mortality and morbidity across the globe, often arising from the consumption of contaminated food and water sources. Approximately 2.2 billion individuals worldwide lack access to improved drinking water services; moreover, about 4.2 billion people do not have access to safely managed sanitation services, and approximately 3 billion individuals lack basic hand washing facilities.[2] Consequently, diarrheal disease caused by infection is widely prevalent throughout developing countries. Diarrhea typically manifests as a symptom of an infection in the intestinal tract, which can be caused by a diverse array of bacterial, viral, and parasitic organisms. Such infections tend to spread through the consumption of contaminated food or drinking water, or via person-to-person transmission resulting from inadequate hygiene practices.[3] Giardiasis is a significant cause of diarrheal disease and a major public health concern, particularly in developing countries where access to clean water and sanitation is limited.[4-6]

*Corresponding author: Nasser Samadzadehaghdam, Email: nsamadzadeh_a@yahoo.com

According to the World Health Organization (WHO), *Cryptosporidium* and *Giardia* are protozoa parasites that are commonly found in contaminated drinking water and food. Contaminated drinking water is a major source of the spread of diseases such as diarrhea, cholera, dysentery, typhoid, and polio. Despite undergoing various chemical and filtration processes during water treatment, these parasites can still survive and cause illness in individuals who come into contact with them. It is therefore critical to develop effective methods to detect and remove these parasites from drinking water to ensure public health and safety.[7, 8]

Giardia lamblia is a microscopic flagellated parasite that causes diarrhea, with 280 million cases per year.[9] It has two life forms: motile trophozoite and non-motile cyst. It is transmitted through ingestion of viable cysts from water, food, and the fecal-oral route. *Giardia* infection can range from asymptomatic to severe diarrhea, malabsorption, and failure to thrive. Diagnosis is done through microscopic detection of diagnostic stages in fecal samples, coproantigen detection, and molecular techniques. Chemotherapy and disease control methods will always be required as eradicating human *Giardia* infections is unlikely.[9] However, abnormality detection and classification through visual inspection of microscopic images can be time-consuming and prone to human errors.

Related Works

Recently, automatic methods based on artificial intelligence have gained significant attention as more efficient and accurate alternatives. The progress in machine learning technology has led to remarkable advancements in various domains, such as image classification, object detection, semantic segmentation, decision-making, and more, through the application of deep learning techniques.[10-15] Meanwhile, deep learning models, which are inspired by human neurons and composed of dense and complex neural layers, have expanded their reach to the domain of medical imaging, resulting in significant improvements in computer-aided detection (CADe) and diagnosis (CADx), radiomics, and medical image analysis.[16]

Several studies have explored the application of artificial intelligence for parasite detection and classification. To reduce human errors, Widmer et al[17] used artificial neural networks to identify *Cryptosporidium* oocyst and *Giardia* cyst from fluorescent microscopic images captured by a color digital camera at x400 magnification. The correct identification percentage of *Giardia* cysts ranged from 88.6% to 91.8%. Xu et al[18] proposed ParasNet, a fast parasite detection system based on deep convolutional neural networks, demonstrating promising results in cell-level *Cryptosporidium* and *Giardia* detection in drinking water (Giardia detection accuracy: 99.5%). In another study, Luo et al[19] developed a system for the detection of *Cryptosporidium* and *Giardia* in drinking water by combining imaging flow cytometry and MCellNet deep network. This network uses the MobileNet-v2 as its building block and optimizes it to increase processing speed and accuracy for imaging flow cytometry. The network achieved a detection accuracy of 99.6%. In another research, Mathison et al[20] utilized a deep convolutional neural network to detect intestinal protozoa, including *Giardia*, in trichrome-stained stool specimens. Their findings demonstrated the effectiveness of deep learning in enhancing the sensitivity and specificity of parasite detection. Moreover, Luo et al.[21] addressed the challenge of rare bioparticle detection through deep metric learning, which could classify *Giardia* with a high accuracy of 99.86% in drinking water. In a recent paper, Nakarmi et al,[22] investigated the application of smartphone-based microscopy for the detection of *Giardia* and *Cryptosporidium* in vegetable samples using Faster RCNN, RetinaNet, and YOLOv8s models. However, the results demonstrated that deep learning methods perform better with the brightfield microscopy images than the smartphone microscopy image dataset (*Giardia* detection precision: 85.5% obtained by YOLOv8s).

In contrast to most of the previous studies that have detected *Giardia* through analysis of microscopic images of drinking water samples, in this study, we have used microscopic images of stool samples as our machine learning dataset. The aim of this study is the automatic classification of *Giardia lamblia* parasite from three categories including normal, cyst, and trophozoite, based on stool samples, using pre-trained deep learning models for more rapid and accurate diagnosis of cases with giardiasis as a valuable assistant for laboratory science experts and parasitologists. In this study, various models were employed to assess their classification performance, namely Xception, ResNet-50, and EfficientNet-B0. Among these models, EfficientNet-B0 exhibited superior performance compared to the others.

Materials and Methods

Database

To gather the necessary dataset, a collaborative effort was undertaken with the parasitology and mycology group at the School of Medicine, Tabriz University of Medical Sciences. This research study involved the collection of data from both positive cases of giardiasis and normal samples, specifically focusing on three distinct classes: cyst, trophozoite (affected cases), and normal samples. The collection of slides was carried out using two different methods. For the cyst and normal classes, slides were prepared through the direct expansion method using samples that were stored at temperatures below zero degrees. On the other hand, for trophozoite samples, prestained Giemsa slides were utilized. The slides were

examined under the Nikon YS100 microscope with ×40 magnification factor and the images were captured using a Xiaomi Poco M3 smartphone with a resolution of 2340×1080 pixels. A total number of 1610 image data from stool samples were collected. Out of these, 630 images were attributed to the trophozoite class, 570 images corresponded to the normal class, and the remaining 410 images were associated with cysts.

Preprocessing

In contrast to previous studies that used microscopic images of drinking water samples, in this study, the microscopic images of stool samples are used all of which have significant artifacts and noise due to the presence of intestinal bacteria and fecal matter. The crowded microscopic field resulting from intestinal bacteria and excreted food makes it much harder to identify the parasite compared to drinking water samples. Therefore, to better visualize the parasite in both cyst and trophozoite forms preprocessing is necessary. Before preprocessing, images are converted to grayscale and cropped in size of 1840×1840 to remove the dark margins outside the microscope field of view; then resized to 512×512 pixels to reduce the computational burden of the deep network. The contrast of the images is enhanced in two steps by applying contrast limited adaptive histogram equalization (CLAHE) and a Gabor filter. In the following, these two methods are briefly explained.

Local Histogram Equalization (CLAHE) is a computer vision technique used to enhance the contrast of an image by normalizing the intensity values of small local regions within the image. This technique is particularly useful for images with low contrast or uneven lighting conditions. CLAHE works by dividing the image into small square regions called tiles and computing a histogram of the pixel intensities for each tile. The histogram is then equalized using a modified form of the cumulative distribution function (CDF) that limits the maximum and minimum values of the histogram to avoid amplifying noise. The resulting equalized histogram is used to map the pixel intensities in the tile to a new range of values that better utilizes the available dynamic range of the image. The use of CLAHE has been shown to enhance the contrast and improve the visibility of fine details in images from various domains, including medical imaging, remote sensing, and microscopy.[23] We applied CLAHE to enhance the contrast of the images and improve the visibility of the parasites.

The Gabor filter is a linear filter used in image processing and computer vision to enhance edges and textures in an image by analyzing its spatial frequency and orientation. It is a complex-valued filter that combines a sinusoidal wave with a Gaussian envelope. A complex 2D Gabor filter in the image domain (x,y) is defined as[24]:

$$g\left(x,y,\theta_k,f,\sigma_x,\sigma_y\right)=\exp\left(-\frac{1}{2}\left(\frac{{x_{\theta_k}}^2}{\sigma_x^2}+\frac{{y_{\theta_k}}^2}{\sigma_y^2}\right)\right)\times\exp\left(2\pi i f x_{\theta_k}\right) \quad (1)$$

$$x_{\theta_k}=x\cos\theta_k+y\sin\theta_k \;\; and \;\; y_{\theta_k}=-x\sin\theta_k+y\cos\theta_k \quad (2)$$

Where f is the frequency of the sinusoidal plane wave, θ is the orientation of the Gabor filter, and σ_x and σ_y are the standard deviations of the Gaussian envelope along the x and y axes, respectively. We applied a Gabor filter with specific parameters to suppress the noise and enhance the features of the images. Three samples of images and their preprocessed versions are shown in Fig. 1.

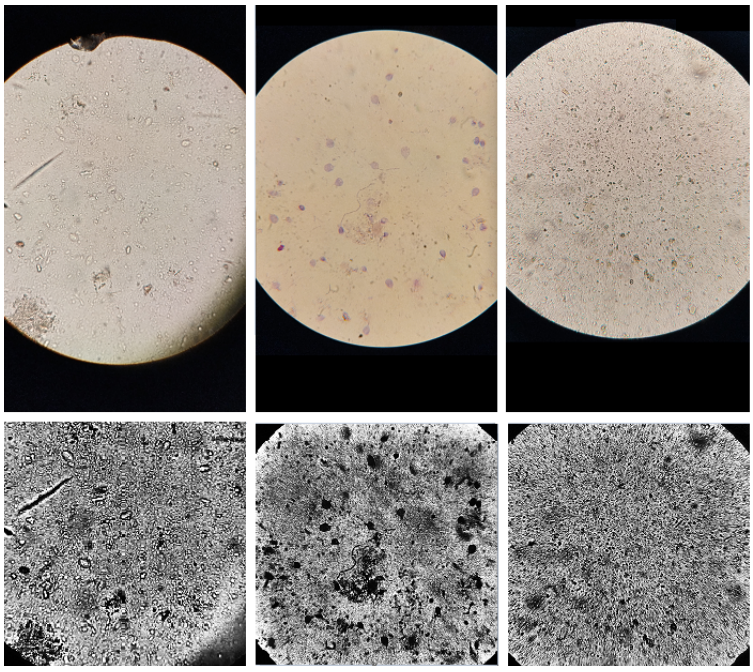

Fig. 1. Top row: raw images, bottom row: preprocessed images. Left: cyst, middle: trophozoite, right: normal

Convolutional neural networks

Convolutional neural network (CNN) is a type of deep learning model that utilizes multiple layers for feature extraction and image classification. The CNN architecture has been widely studied and has shown significant performance improvements in various computer vision tasks.[25,26] Deep learning and CNNs have shown significant promise in the classification and analysis of microscopic images. CNN-based methods effectively identify subtle features in microscopic images that are challenging for human analysts to discern.[27-29] In this case, we employed CNNs to classify the microscopic images into different *Giardia* cases and normal samples. Several CNN architectures, including Xception, ResNet-50, and EfficientNet-B0, were trained using the Keras deep learning library. We utilized transfer learning to initialize the weights of the CNNs with pre-trained models on the ImageNet dataset. The last few layers of the pre-trained models were fine-tuned on our dataset to adapt them to the specific task of Giardia classification.

Xception

Xception is a deep convolutional neural network architecture introduced by Chollet in 2017 as an extension of the Inception architecture.[30] It is based on the concept of depthwise separable convolutions, which split the standard convolution operation into two separate operations: a depthwise convolution and a pointwise convolution. This approach reduces the computational cost of convolutions while still capturing crucial features in the input data. It enables more efficient utilization of model parameters, leading to a more accurate and efficient model.[30,31] Xception has demonstrated superior performance compared to other popular neural network architectures like ResNet and Inception on various benchmark image classification datasets, including ImageNet and CIFAR-10. Additionally, Xception has fewer parameters than these architectures, resulting in improved computational efficiency. The adaptability of the Xception architecture extends to different computer vision tasks, including object detection, semantic segmentation, and style transfer, among others. It has become a popular choice for image recognition tasks in both academia and industry due to its high accuracy and efficiency.[30]

ResNet-50

ResNet50 is a specific ResNet architecture introduced by He et al. in 2015.[32] It consists of 50 layers and is trained using the stochastic gradient descent optimizer. ResNet50 consists of 50 convolutional layers, including shortcut connections that allow the network to bypass one or more layers, making it possible to train deeper networks without encountering the vanishing gradient problem. The ResNet architecture was developed to address the problem of degradation that occurs when adding more layers to a neural network. As the number of layers in a network increases, the performance of the network on the training set starts to saturate and then degrade rapidly. This degradation is caused by the vanishing gradient problem, which occurs when the gradients become very small as they propagate through the layers of the network, making it difficult to update the weights of the lower layers. To overcome this problem, ResNet introduced the concept of residual learning, where the output of a layer is added to the input of one or more subsequent layers, allowing the network to learn residual functions instead of learning the underlying mapping directly. This approach facilitates the training of deeper networks because the gradients can flow directly through the shortcut connections, bypassing the problematic layers. ResNet50 has been widely used in various computer vision tasks, such as image classification, object detection, and semantic segmentation, and has achieved state-of-the-art results on many benchmark datasets.[26]

EfficientNet-B0

EfficientNet-B0 is a CNN architecture introduced by Tan et al in 2019.[31] It represents a significant advancement in the realm of deep learning, achieving state-of-the-art performance while being computationally efficient. EfficientNet-B0 employs a compound scaling method that systematically scales up the depth, width, and resolution of the network. This scaling approach allows EfficientNet-B0 to strike a balance between accuracy and efficiency. The network utilizes depth-wise separable convolutions, which split the standard convolutional operation into separate depth-wise and point-wise convolutions, reducing the number of parameters and computational cost. It also incorporates batch normalization, Swish activation function, dropout regularization, and squeeze-and-excitation blocks to enhance its performance and generalization capabilities. The compound scaling method of EfficientNet-B0 enables it to efficiently scale up or down to different model sizes, making it adaptable to a wide range of computational resources and accuracy requirements. EfficientNet-B0 has been extensively evaluated on benchmark datasets like ImageNet, consistently achieving top-tier performance.

Training and Evaluation

To address the data requirements of deep learning models, we employed data augmentation techniques to augment the dataset, enhance its diversity, and mitigate overfitting. In this regard, we used several data augmentation techniques, including random rotations, zooms, shifts, flips, shears, and fill modes. They effectively increased the dataset's size and diversity, while also preventing overfitting. By applying these augmentation techniques, the model was trained to identify objects or patterns in varying orientations, sizes, and lighting conditions, and it became more robust to variations in the input data.

In this study, an 80/20 train-test split was utilized

to train and evaluate the performance of the CNNs. The stochastic gradient descent (SGD) optimizer was employed during the training process with a learning rate of 0.002 and a batch size of 20. The training of the models was conducted for 25 epochs. To prevent overfitting of the model during the learning process, techniques such as dropout, early stopping, and batch normalization were employed.

Results

The performance of the three models was evaluated on the test subset using multiple metrics, including precision, accuracy, recall, F1 score, and the loss function value. Fig. 2 displays the loss values for both training and validation datasets. As depicted, the training loss values decrease over epochs for all models. Based on the loss function graphs of the trained models, it can be observed that EfficientNet-B0 and Xception exhibited lower oscillation compared to ResNet-50. This indicates that learning was performed more effectively in the former models.

The quantitative criteria for evaluating model performance include: accuracy, recall, precision, F_1-score, and the loss function value. The relevant formulae are given by the following equations:

$$Precision = \frac{1}{C}\sum_{i=1}^{C}\frac{TP_i}{TP_i + FP_i} \quad (3)$$

$$Accuracy = \sum_{i=1}^{C}\frac{TP_i}{TP_i + TN_i + FP_i + FN_i} \quad (4)$$

$$Recall = \frac{1}{C}\sum_{i=1}^{C}\frac{TP_i}{TP_i + FN_i} \quad (5)$$

$$Specificity = \frac{1}{C}\sum_{i=1}^{C}\frac{TN_i}{TN_i + FP_i} \quad (6)$$

$$F_1 = \frac{1}{C}\sum_{i=1}^{C}\frac{2TP_i}{2TP_i + FP_i + FN_i} \quad (7)$$

Where, T and F stand for true and false, and subscripts P and N denote positive and negative results of classification, respectively. C is the number of classes that is equal to three here.

Moreover, confusion matrices were generated to visualize the performance of the models in classifying the *Giardia* and normal samples (Fig. 3). Using theses matrices and the aforementioned formula, the evaluation metrics are computed and summarized in Table 1.

The results obtained indicate that, among the models used for classification, EfficientNet-B0 was less prone to overfitting compared to the other two models and achieved better learning performance than the other two.

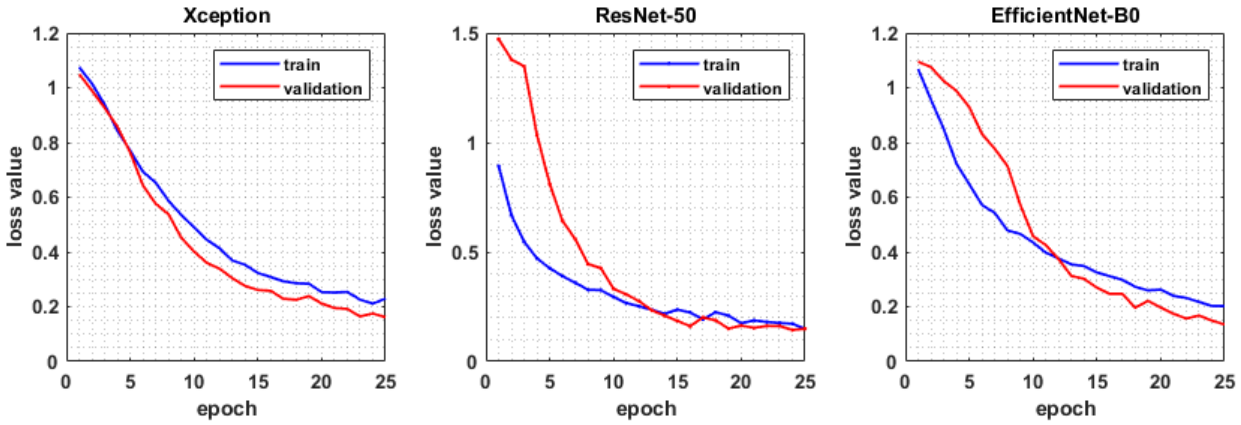

Fig. 2. The value of loss function for training and test data through 25 epochs.

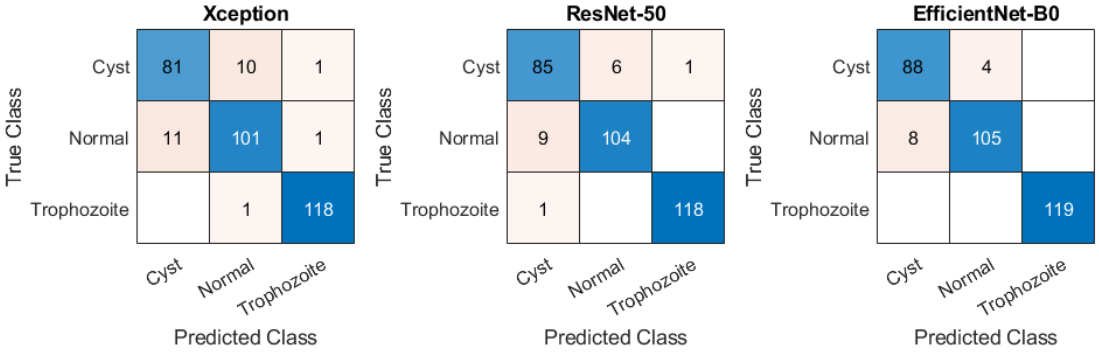

Fig. 3. Confusion matrices obtained for each of the models.

Discussion

In this research, we employed the potential of artificial intelligence to discriminate between two life cycles of *Giardia lamblia*, namely the cyst and trophozoite, as well as the normal case. The methodology involved the acquisition of high-resolution digital microscopic images, followed by a preprocessing step. Subsequently, these images were utilized as input for three deep neural networks, with the EfficientNet-B0 model demonstrating exceptional performance in the three-class classification task. The results obtained from the model were highly impressive, with a training accuracy of 95.33% and a validation accuracy of 96.29% achieved after 30 epochs. The observation that the validation accuracy surpasses the training accuracy indicates that the model is not overfitting to the training data. Moreover, the consistently decreasing loss values throughout the epochs further signify that the model's predictive capabilities are continuously improving.

Table 2 compares studies that addressed the automatic detection of *Giardia*. Notably, the majority of these studies focused on detecting *Giardia* from water samples by methods other than conventional light microscopy. Among these studies, the detection accuracy is relatively high, approximately 99%. However, in comparison to the findings reported in Nakarmi et al,[22] the EfficientNet-B0 model reaches a 10% higher precision value. The present study bears more resemblance to Mathison et al[20] since both have considered the trophozoite and cyst life cycles of *Giardia*. Nonetheless, considering the number of images per class and the variety of parasites or particles included, the scope of the current study is relatively limited. Despite these limitations, achieving a validation accuracy of 96.29% in a classification problem is remarkably high. This outcome underscores the effectiveness of the EfficientNet-B0 model in discerning between the three classes under investigation. Consequently, the findings

Table 1. The classification evaluation of the networks obtained for the test data

	Precision (%)	Accuracy (%)	Recall (%)	Specificity (%)	F_1-score (%)
Xception	92.18	92.59	92.19	96.35	92.18
ResNet-50	94.39	94.75	94.52	97.45	94.44
EfficientNet-B0	95.99	96.29	96.19	98.21	96.07

Table 2. Summary of the studies on *Giardia* detection by artificial intelligence methods

Reference	Imaging Method	Dataset Details	Classification Method	Number of classes	Evaluation metrics
[17]	Fluorescent microscopy of water	Cryptosporidium oocyst: 2,086 images Giardia cyst: 2,713 images	Artificial neural networks	2	Cryptosporidium oocyst: Accuracy: 91.8% Giardia cyst: Accuracy: 98.9%
[18]	Bright field microscopy of drinking water	Cryptosporidium: 5,000 images Giardia: 5,000 images Other particles: 5,000 images	Deep convolutional neural network: ParasNet	3	Cryptosporidium: Accuracy: 95.6% Giardia: Accuracy: 99.5%
[19]	Imaging flow cytometry of drinking water	Cryptosporidium: 2,082 images Giardia: 3,569 images Beads with different sizes: 46,669 images Natural pollutants: 27,826 images	MCellNet	13	Accuracy: 99.69% Precision: 99.67% Recall: 99.41% F1-score: 99.54%
[21]	Imaging flow cytometry of drinking water	Cryptosporidium: 2,078 images Giardia: 3,438 images Natural pollutants: 84,147 images	Deep metric learning	3	Accuracy: 99.86% Precision. 98.84% Recall: 99.17% F1-score: 99.00%
[20]	Light microscopy of stool samples	Giardia duodenalis cyst: 6,499 Giardia duodenalis trophozoite: 2,191 Others: 78,040	a Deep Convolutional Neural Network	11	Accuracy was calculated as slide-level agreement (e.g., parasite present or absent) with microscopy. Positive agreement was 98.88% (95% confidence interval, 93.76% to 99.98%), and negative agreement was 98.11% (95% CI, 93.35% to 99.77%)
[22]	Brightfield microscopy of reference oocyst suspension samples and vegetable samples	Cryptosporidium oocyst: 1,242 images Giardia oocyst: 1,251 images	YOLOv8s	2	Giardia: Precision: 85.5%; Recall: 81.1%; F1-score: 83.1% Cryptosporidium: Precision: 87.9%; Recall: 71.6%; F1-score: 78.8%
Current study	Light microscopy of stool samples	Giardia Cyst: 410 images Giardia Trophozoite: 630 images Normal samples: 570 images	EfficientNet-B0	3	Accuracy: 96.29% Precision: 95.99% Recall: 96.19% Specificity: 98.21% F1-score: 96.07%

Research Highlights

What is the current knowledge?

- Most of the studies have concentrated on Giardia classification in water samples.

What is new here?

- Giardia classification based on stool microscopic images is achieved by deep neural networks.

of this study strongly suggest that the utilization of the EfficientNet-B0 model is an appropriate choice for addressing this particular classification task.

Conclusion

In conclusion, our research leveraged the potential of artificial intelligence to successfully discriminate between the cyst, trophozoite, and normal life cycles of *Giardia lamblia*. The implementation of the EfficientNet-B0 model yielded outstanding results, with high accuracies achieved in both training and validation phases. These findings support the suitability of the EfficientNet-B0 model for accurate classification in this domain. Moving forward, further investigations could explore the generalizability of the model on larger datasets and its potential application in clinical settings for the identification and diagnosis of *Giardia lamblia* life cycles.

Acknowledgments

We would like to thank the parasitology and mycology group at the School of Medicine, Tabriz University of Medical Sciences for providing the dataset used in this study.

Authors' Contribution

Conceptualization: Nasser Samadzadehaghdam, Ehsan Ahmadpour.
Data curation: Pezhman Yarahmadi, Ehsan Ahmadpour.
Formal analysis: Pezhman Yarahmadi.
Funding acquisition: Nasser Samadzadehaghdam.
Investigation: Pezhman Yarahmadi, Nasser Samadzadehaghdam, Ehsan Ahmadpour.
Methodology: Pezhman Yarahmadi, Nasser Samadzadehaghdam, Parham Moradi.
Software: Pezhman Yarahmadi, Parham Moradi.
Supervision: Nasser Samadzadehaghdam, Ehsan Ahmadpour.
Validation: Pezhman Yarahmadi, Nasser Samadzadehaghdam, Ehsan Ahmadpour.
Writing–original draft: Pezhman Yarahmadi, Nasser Samadzadehaghdam.
Writing–review & editing: Nasser Samadzadehaghdam, Pezhman Yarahmadi, Ehsan Ahmadpour, Parham Moradi.

Competing Interests

The authors declare no conflict of interest.

Ethical Statement

This study was conducted in accordance with the ethical guidelines provided by the Research Ethics Committee of Tabriz University of Medical Sciences with the ethical code number IR.TBZMED.VCR.REC.1400.428.

Funding

This research is part of a MSc. thesis supported financially by Tabriz University of Medical sciences under grant no: 68727.

References

1. Shine S, Muhamud S, Adanew S, Demelash A, Abate M. Prevalence and associated factors of diarrhea among under-five children in Debre Berhan town, Ethiopia 2018: a cross-sectional study. *BMC Infect Dis* **2020**; 20: 174. doi: 10.1186/s12879-020-4905-3.
2. World Health Organization (WHO). 1 in 3 People Globally Do Not Have Access to Safe Drinking Water – UNICEF, WHO; **2019**. Available from: https://www.who.int/news/item/18-06-2019-1-in-3-people-globally-do-not-have-access-to-safe-drinking-water-unicef-who.
3. World Health Organization (WHO). Diarrhoeal Disease. WHO; **2017**. Available from: https://www.who.int/news-room/fact-sheets/detail/diarrhoeal-disease.
4. Ryan U, Cacciò SM. Zoonotic potential of *Giardia*. *Int J Parasitol* **2013**; 43: 943-56. doi: 10.1016/j.ijpara.2013.06.001.
5. Thompson RC. Giardiasis as a re-emerging infectious disease and its zoonotic potential. *Int J Parasitol* **2000**; 30: 1259-67. doi: 10.1016/s0020-7519(00)00127-2.
6. Savioli L, Smith H, Thompson A. Giardia and *Cryptosporidium* join the 'neglected diseases initiative'. *Trends Parasitol* **2006**; 22: 203-8. doi: 10.1016/j.pt.2006.02.015.
7. World Health Organization (WHO). *Progress on Drinking Water, Sanitation and Hygiene: 2017 Update and SDG Baselines*. WHO; **2017**.
8. World Health Organization (WHO). *Drinking Water Factsheets*. Geneva: WHO; **2017**.
9. Shalaby NM, Wakid MH. Giardiasis in man: review and updates. *JKAU Med Sci* **2014**; 21: 81-94. doi: 10.4197/Med.21-1.6.
10. LeCun Y, Bengio Y, Hinton G. Deep learning. *Nature* **2015**; 521: 436-44. doi: 10.1038/nature14539.
11. Ding H, Jiang X, Liu AQ, Thalmann NM, Wang G. Boundary-aware feature propagation for scene segmentation. In: *Proceedings of the IEEE/CVF International Conference on Computer Vision*. IEEE; **2019**. doi: 10.1109/iccv.2019.00692.
12. Ding H, Jiang X, Shuai B, Liu AQ, Wang G. Semantic correlation promoted shape-variant context for segmentation. In: *Proceedings of the IEEE/CVF Conference on Computer Vision and Pattern Recognition*. IEEE; **2019**. doi: 10.1109/tip.2019.2962685.
13. Ding H, Jiang X, Shuai B, Liu AQ, Wang G. Context contrasted feature and gated multi-scale aggregation for scene segmentation. In: *Proceedings of the IEEE Conference on Computer Vision and Pattern Recognition*. IEEE; **2018**. doi: 10.1109/cvpr.2018.00254.
14. Shuai B, Ding H, Liu T, Wang G, Jiang X. Towards achieving robust low-level and high-level scene parsing. *IEEE Trans Image Process* **2018**; 28: 1378-90. doi: 10.1109/tip.2018.2878975.
15. Ding H, Jiang X, Shuai B, Liu AQ, Wang G. Semantic segmentation with context encoding and multi-path decoding. *IEEE Trans Image Process* **2020**; 29: 3520-33. doi: 10.1109/tip.2019.2962685.
16. Suzuki K. Overview of deep learning in medical imaging. *Radiol Phys Technol* **2017**; 10: 257-73. doi: 10.1007/s12194-017-0406-5.
17. Widmer KW, Srikumar D, Pillai SD. Use of artificial neural networks to accurately identify *Cryptosporidium* oocyst and *Giardia* cyst images. *Appl Environ Microbiol* **2005**; 71: 80-4. doi: 10.1128/aem.71.1.80-84.2005.
18. Xu XF, Talbot S, Selvaraja T. ParasNet: fast parasites detection with neural networks. ArXiv [Preprint]. February 26, **2020**. Available from: https://arxiv.org/abs/2002.11327.
19. Luo S, Nguyen KT, Nguyen BT, Feng S, Shi Y, Elsayed A, et al. Deep learning-enabled imaging flow cytometry for high-speed *Cryptosporidium* and *Giardia* detection. *Cytometry* A **2021**; 99: 1123-33. doi: 10.1002/cyto.a.24321.
20. Mathison BA, Kohan JL, Walker JF, Smith RB, Ardon O, Couturier MR. Detection of intestinal protozoa in trichrome-stained stool specimens by use of a deep convolutional neural network. *J Clin Microbiol* **2020**; 58: e02053-19. doi: 10.1128/jcm.02053-19.
21. Luo S, Shi Y, Chin LK, Zhang Y, Wen B, Sun Y, et al. Rare bioparticle detection via deep metric learning. *RSC Adv* **2021**; 11: 17603-10. doi: 10.1039/d1ra02869c.
22. Nakarmi S, Pudasaini S, Thapaliya S, Upretee P, Shrestha R, Giri

B, et al. Deep-learning assisted detection and quantification of (oo) cysts of *Giardia* and *Cryptosporidium* on smartphone microscopy images. ArXiv [Preprint]. April 11, **2023**. Available from: https://arxiv.org/abs/2304.05339.
23. Pizer SM, Amburn EP, Austin JD, Cromartie R, Geselowitz A, Greer T, et al. Adaptive histogram equalization and its variations. *Computer Vision, Graphics, and Image Processing* **1987**; 39: 355-68. doi: 10.1016/s0734-189x(87)80186-x.
24. Lee CJ, Wang SD. Fingerprint feature extraction using Gabor filters. *Electron Lett* **1999**; 35: 288-90. doi: 10.1049/el:19990213.
25. LeCun Y, Bottou L, Bengio Y, Haffner P. Gradient-based learning applied to document recognition. *Proc IEEE* **1998**; 86: 2278-324. doi: 10.1109/5.726791.
26. Hinton GE, Srivastava N, Krizhevsky A, Sutskever I, Salakhutdinov RR. Improving neural networks by preventing co-adaptation of feature detectors. ArXiv [Preprint]. July 3, **2012**. Available from: https://arxiv.org/abs/1207.0580.
27. Wang D, Khosla A, Gargeya R, Irshad H, Beck AH. Deep learning for identifying metastatic breast cancer. ArXiv [Preprint]. 2016 June 18, **2016**. Available from: https://arxiv.org/abs/1606.05718.
28. Rajaraman S, Antani SK, Poostchi M, Silamut K, Hossain MA, Maude RJ, et al. Pre-trained convolutional neural networks as feature extractors toward improved malaria parasite detection in thin blood smear images. *PeerJ* **2018**; 6: e4568. doi: 10.7717/peerj.4568.
29. Ekins S, Puhl AC, Zorn KM, Lane TR, Russo DP, Klein JJ, et al. Exploiting machine learning for end-to-end drug discovery and development. *Nat Mater* **2019**; 18: 435-41. doi: 10.1038/s41563-019-0338-z.
30. Chollet F. Xception: deep learning with depthwise separable convolutions. In: *Proceedings of the IEEE Conference on Computer Vision and Pattern Recognition*. IEEE; **2017**. doi: 10.1109/cvpr.2017.195.
31. Tan M, Le Q. Efficientnet: rethinking model scaling for convolutional neural networks. In: *International Conference on Machine Learning*. PMLR; **2019**. doi: 10.48550/arXiv.1905.11946.
32. He K, Zhang X, Ren S, Sun J. Deep residual learning for image recognition. In: *Proceedings of the IEEE Conference on Computer Vision and Pattern Recognition*. IEEE; **2016**. doi: 10.1109/cvpr.2016.90.